Volume 1 | Number 1 | Jan 2013 | Pages 1–100

PCCP

Physical Chemistry Chemical Physics
www.rsc.org/pccp

ROYAL SOCIETY OF CHEMISTRY

ROYAL SOCIETY OF CHEMISTRY

www.rsc.org/pccp

Sc$_2$S@C$_{68}$: an Obtuse Di-scandium Sulfide Cluster Trapped in a C_{2v} Fullerene Cage†

Yi-Jun Guo[a,§], **Bo-Chao Gao**[a,§], **Tao Yang**[a], **Shigeru Nagase**[b], **and Xiang Zhao**[*a]

[a]*Institute for Chemical Physics & Department of Chemistry, State Key Laboratory of*

Electrical Insulation and Power Equipment, Xi'an Jiaotong University, Xi'an 710049,

China

Email: xzhao@mail.xjtu.edu.cn; *Fax: +86 29 8266 8559; Tel: +86 29 8266 5671*

[b]*Fukui Institute for Fundamental Chemistry, Kyoto University, Kyoto 606-8103,*

Japan

[§]*These authors contributed equally to this work.*

† Electronic supplementary information (ESI) available: relative energies of selected
C$_{68}$$^{2-}$ and C$_{68}$$^{4-}$ anions at AM1 and B3LYP/6-31G(d) levels of theory, relative energies
and HOMO-LUMO gaps of all selected Sc$_2$S@C$_{68}$ isomers, and simulated ^{13}C NMR
and UV-vis-NIR spectrum as well as Cartesian coordinate of Sc$_2$S@C_{2v}(6073)-C$_{68}$.

Abstract

The spectrum detected smallest sulfide clusterfullerene $Sc_2S@C_{68}$ has not been characterized yet. Herein, we explored a series of $Sc_2S@C_{68}$ species to determine which could be the most promising isomer. The results suggest that a sulfide cluster encapsulated in the $C_{2v}(6073)$-C_{68} cage which violates isolated pentagon rule (IPR) with two opposite pentalenes has the lowest energy and an overwhelming thermodynamic stability. Two scandium atoms coordinate with the two opposite pentalenes, leading to an obtuse Sc-S-Sc angle of 151°. The bond lengths of the two Sc-S bonds are equivalent. Frontier molecular orbital distributions exhibit substantial overlaps between metallic orbitals and cage orbitals, indicating covalent interactions cannot be ignored, which have been unambiguously identified in terms of Mayer bond order and bonding critical point (BCP) indicators methods. Electrochemical properties as well as ^{13}C NMR, UV-vis-NIR, and IR spectra of $Sc_2S@$ $C_{2v}(6073)$-C_{68} have been theoretically studied to assist further experimental characterization.

1. Introduction

Metal atoms or metallic cluster can be encapsulated by fullerene cages forming endohedral metallofullerenes (EMFs).[1] One of attractive features of EMFs is the formal electron transfer from metallic valence orbitals to frontier orbitals of fullerene cage, which changes the electronic properties of fullerenes. As a result, a series of unstable pristine fullerene cages of which some violate the well-known isolated pentagon rule (IPR)[2] can be stabilized. Some representative examples are $Sc_2@C_{66}$,[3] $Sc_2@C_{70}$,[4] $Sc_2C_2@C_{72}$,[5] and $M_2C_2@C_{84}$ (M = Y[6] and Gd[7]).

As a consequence of no IPR-obeying isomers, it seems impossible to synthesize any neutral pristine C_{68} isomers. In order to take a glance of the properties of C_{68} fullerene, study on its endohedral derivatives including experimental and theoretical methods becomes particularly important. As the first metallic clusterfullerene violating IPR, $Sc_3N@D_3(6140)-C_{68}$ has got tremendous attention[8-12] since it was isolated in the year of 2000.[13] At the same time, structure argument[14] on the most stable Sc_2C_{70} isomer, a carbide cluster fullerene $Sc_2C_2@C_{68}$[15] or a di-metal fullerene $Sc_2@C_{70}$,[4] makes the C_{68} fullerene more fascinating.

Recently, a new kind of EMFs called sulfide clusterfullerene was discovered, which contains one sulfide and two metal atoms. Dunsch et al. isolated such kind of EMFs, $M_2S@C_{82}$ (M = Sc, Y, Dy, and Lu)[16], for the fist time in 2010. Later, two $Sc_2S@C_{82}$ isomers were unambiguously characterized as $Sc_2S@C_S(6)-C_{82}$ and $Sc_2S@C_{3v}(8)-C_{82}$[17] by single-crystal X-ray diffraction analysis. So far, an extensive family of novel scandium sulfide cluster fullerenes with cages ranging from C_{68} to

C_{100} can be obtained in macroscopic quantities by introducing SO_2 into the arc reactor.[18,19] X-ray crystallographic characterization revealed that the isolated $Sc_2S@C_{72}$ isomer[19] possesses the extraordinary C_s(10528) cage with two pairs of pentalene units. Very recently, two independent groups[20,21] reported that the cage structure of $Sc_2S@C_{70}$ was not the conventional D_{5h} but the C_2(7892) symmetry with two pairs of pentagon adjacencies.

Herein, we report systematical density functional theory (DFT) investigations on the geometry and electronic structure of di-metallic sulfide clusterfullerene $Sc_2S@C_{68}$ which is the smallest discandium sulfide fullerene detected by mass spectra so far without any other characterizations.[19] Our reliable computations demonstrate that the C_{2v}(6073)-C_{68} which violates the IPR with two pairs of pentagon adjacencies is utilized to encapsulate a di-scandium sulfide cluster. Meanwhile, their intracluster as well as cluster-cage bonding natures, redox properties and electronic absorption, infrared, and ^{13}C NMR spectra of the $Sc_2S@C_{68}$ were also computed and simulated theoretically. All of those calculated properties may provide an important guidance for the future deeply experimental characterization.

2. Computational Details

As we are aware, since both +2 and +3 are normal valence states of a scandium atom, the valence state of Sc atoms in different fullerene cavities has been argued for a long time. For example, Pichler et al. declared some proofs for formal Sc^{3+} cations in $Sc_2@C_{84}$,[22] while a recent progress suggests that the formal valence state of $Sc_2@C_{70}$ should be $(Sc^{2+})_2(C_{70})^{4-}$.[4] In order to consider comprehensively, both the di-

and tetra- anions of 2636 C_{68} isomers[2] with no more than six pairs of pentagon adjacencies were selected at the very beginning of the present work.

All the di- and tetra- anions of C_{68} isomers were firstly screened at the AM1[23] level to evaluate the energetics (See Table S1 and Table S2 in the Supplementary Information). Next, some relatively low-energy anions were further optimized at the hybrid density functional B3LYP[24] level with 6-31G(d) basis set (see Table S3 and Table S4). Then, a two-step geometry optimization of $Sc_2S@C_{68}$ isomers was performed with the same B3LYP density functional. The d-polarized splitting valence 6-31G(d) basis set was used for C and S atoms, and the Lanl2dz[25] basis set with the corresponding effective core potential was used for Sc atoms. To gain the global minimum on the potential energy surface, several different orientations of the endohedral Sc_2S clusters were taken into consideration. A detailed description on the optimization process has been stated in the ESI†. At last, the top-six energy-lowest $Sc_2S@C_{68}$ isomers were reoptimized at a higher B3LYP/6-311G(d)~SDD[26] (6-311G(d) basis set for C and S atoms and SDD basis set for Sc atoms).

All stationary points were verified as minima by vibrational frequency analysis at the B3LYP/3-21G*~CEP-31G level. Based on the frequency analysis, rotational-vibrational partition functions can also be gained, and the entropy effects of $Sc_2S@C_{68}$ isomers can be taken into accounts for their thermodynamic stability according to the following formula.[27]

$$w_i = \frac{q_i \exp[-\Delta H_{0,i}^O/(RT)]}{\sum_{j=1}^m q_j \exp[-\Delta H_{0,j}^O/(RT)]} \tag{1}$$

where R is the gas constant and T is the absolute temperature. eq 1 is an exact

relationship derived from the principle of equilibrium statistical thermodynamics, that is, from the standard Gibbs energies of isomers, and it is strongly temperature dependent. Considering the entropy effects to determine to most thermodynamically stable isomer is necessary since the temperature region of fullerene formation is rather high. A series of published papers[28-32] have shown that it is an effective and reliable method to evaluate thermodynamic stabilities of EMFs at relatively high temperature region where fullerene formation reactions take place. All of the DFT calculations mentioned above were performed using the Gaussian09 program package.[33]

To investigate bonding natures of $Sc_2S@C_{2v}(6073)\text{-}C_{68}$, Mayer bond orders[34-36] and bonding critical point (BCP) indicators[37] of $Sc_2S@C_{2v}(6073)\text{-}C_{68}$ have been examined by using MUlTIWFN 3.2.1 program.[38]

The electrochemical redox potentials were evaluated by using a conductor-like screening model (COSMO)[39] at the PBE/DNP level in the Dmol3 code[40]. o-Dichlorobenzene (o-DCB; dielectric constant $= 10.12$) was chosen as the solvent. The geometries and total energies of $[Sc_2S@C_{2v}(6073)\text{-}C_{68}]^q$ ($q = 0,\ \pm1,$ and ±2) in the solvent were computed. The redox reaction in the solvent can be expressed simply as the reduced form (solvent) $\rightarrow$ oxidized form (solvent) $+ e$. The computed redox potential E^0 can be defined in the following form:

$$E^0 = \Delta G - 4.98 \text{ (eV)} \tag{1}$$

where ΔG is the free energy change of the above reaction and is approximated by the total electronic energy change of the reaction, and 4.98 (eV) is the free energy change associated with the reference ferrocene/ferrocenium (Fc/Fc$^+$) redox couple.[41] This

method has been employed to compute redox potentials of EMFs such as $Sc_3C_2@C_{80},$[42] $Sc_4C_2@C_{80},$[43] $Sc_2S@C_{70},$[20] and $Sc_3NC@C_{2n}$ ($2n$ = 68, 70 and 80).[44]

By utilizing Gaussian09 program package, the ^{13}C NMR chemical shifts of $Sc_2S@C_{2v}(6073)$-C_{68} are simulated out at the B3LYP/6-311G(d)~Lanl2dz level of theory with the gauge-independent atomic orbital (GIAO) method. Theoretical chemical shift value have been calibrated to the observed C_{60} line (142.15 ppm).[45]

The electronic absorption and infrared spectra were simulated by time-dependent density functional theory (TD-DFT) and harmonic vibrational analysis respectively. This part of computation was also performed by Gaussian09 program package.

3. Results and Discussion

3.1 Relative energies and thermodynamic stabilities of $Sc_2S@C_{68}$ species

The DFT results disclose that $C_{2v}(6073)$-C_{68} and $C_s(6094)$-C_{68} with two pentagon adjacencies are the most stable tetra- and di- anions of C_{68} isomers, respectively (see Table S3 and S4). Meanwhile, geometry optimizations with B3LYP method on $Sc_2S@C_{68}$ series seems that $Sc_2S@C_{2v}(6073)$-C_{68} possesses the lowest relative energy (Table 1). As a result, a formal four-electron transfer from Sc_2S clusters to the C_{68} cage seems more appropriate than transfer two electrons. $Sc_2S@C_2(6146)$-C_{68} is predicted as the second most stable structure at both B3LYP/6-31G(d)~Lanl2dz and B3LYP/6-311G(d)~SDD levels with approximate 18 kcal/mol energy higher than the ground state. Moreover, the HOMO-LUMO gap of $Sc_2S@C_{2v}(6073)$-C_{68} is 0.28eV larger than that of $Sc_2S@C_2(6146)$-C_{68}, which suggests that $Sc_2S@C_{2v}(6073)$-C_{68} has a better stability of electronic structure. The isomer $Sc_2S@D_3(6140)$-C_{68} which cage

is proper for encapsulating tri-scandium nitride cluster (Sc_3N) is even 21 kcal/mol

more unstable than $Sc_2S@C_{2v}$(6073)-C_{68}. At the same time, the HOMO-LUMO gap

of this isomer is relatively small (less than 1.3 eV). Remarkably, the energy sequence

of $Sc_2S@C_{68}$ isomers is in difference from that of both di- and tetra- C_{68} anions, and

the energy differences among the top-three $Sc_2S@C_{68}$ isomers are much larger than

those among C_{68} anions (both di- and tetra-). Consequently, the classical electron

transfer model seems oversimplified in the description of interactions between the

Sc_2S cluster and C_{2v}(6073)-C_{68} cage.

Table 1. Relative Energies and HOMO – LUMO Gaps of $Sc_2S@C_{68}$ isomers.

| | | | $Sc_2S@C_{68}$ | | | |
| | | | B3LYP/6-31G(d)~Lanl2dz | | B3LYP/6-311G(d)~SDD | |
Spiral ID	Sym.[a]	PA[b]	ΔE [c]	Gap[d]	ΔE [c]	Gap[d]
6073	C_{2v}	2	0.0	1.53	0.0	1.53
6146	C_2	2	17.8	1.25	18.0	1.25
6140	D_3	3	21.6	1.29	20.7	1.29
6039	C_1	3	22.6	1.69	22.7	1.69
6079	C_1	3	23.0	1.72	22.4	1.72
6116	C_1	3	23.0	1.75	22.2	1.76

[a] Symmetry of the original empty cage. [b] The number of pentagon adjacencies (PA). [c] Relative energy (ΔE) units in kilocalories per mole. [d] HOMO-LUMO Gap units in eV.
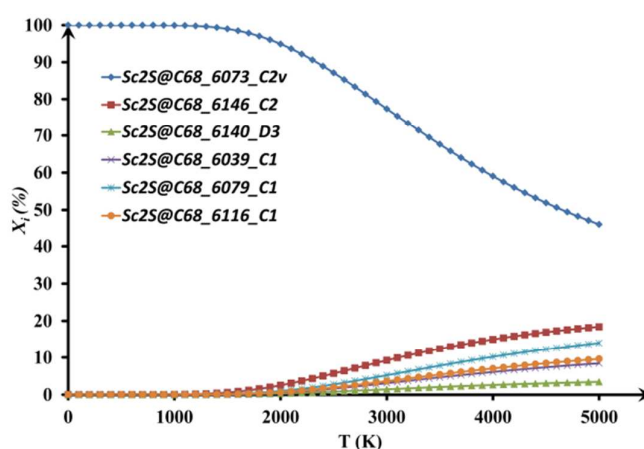

Figure 1. Relative concentrations of the $Sc_2S@C_{68}$ isomers.

The calculated relative concentrations of the top-six lowest-energy $Sc_2S@C_{68}$

isomers in a wide temperature interval are presented in Figure 1. When temperature is below 1000 K, $Sc_2S@C_{2v}(6073)-C_{68}$ is almost the unique product because of its low potential energy. When it is over 1000 K, the concentration of $Sc_2S@C_{2v}(6073)-C_{68}$ starts to decrease, with concentration increase of other five components. Nevertheless, $Sc_2S@C_{2v}(6073)-C_{68}$ keeps overwhelming over the whole calculated temperature range. It turns out that $Sc_2S@C_{2v}(6073)-C_{68}$ exhibits a rather high thermodynamic stability. Comprehensively, for its excellent thermodynamic and kinetic stability of $Sc_2S@C_{2v}(6073)-C_{68}$ among $Sc_2S@C_{68}$ isomers, it can be confirmed undoubtedly that the $Sc_2S@C_{68}$ detected by mass spectrum possesses the $C_{2v}(6073)-C_{68}$ cage. To the best of our knowledge, it is for the first time to confirm a metallic cluster encapsulated by the $C_{2v}(6073)-C_{68}$ cage.

3.2 Geometric and electronic structures

(a)   *(b)*   *(c)*
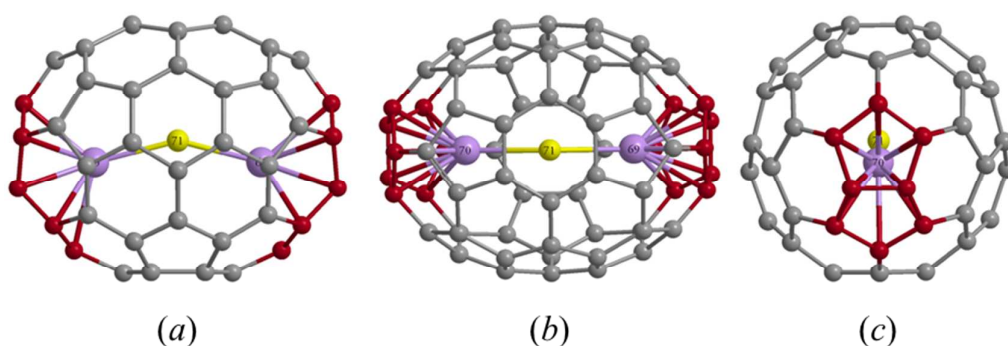
Figure 2. Side(*a*), top(*b*) and left(*c*) views of the optimized $Sc_2S@C_{2v}(6073)-C_{68}$ structure. Those pentalene units, scandium atoms and sulfur atom are colored by vermilion, violet, and bright yellow respectively for emphasis.

As we are aware, there are strong interactions between those two scandium atoms and the pentalene junctions, which are frequently seen in IPR-violating EMFs. In terms of that, it can be inferred that relative locations of fused pentagon adjacencies should influence configurations of the encapsulated metallic cluster. As seen in Figure

2(a), when the cage is viewed orthogonally to the Sc_2S cluster, it is almost elliptical.

Those two fused pentagon adjacencies (highlighted by vermilion) reside on opposite

poles along with its long axis. The separation between the pentalenes is even greater

in $C_{2v}(6073)$-C_{68} (8.56 Å) than in $C_s(10528)$-C_{72} (8.23 Å).[19] Consequently, The

Sc-S-Sc angle in $Sc_2S@C_{2v}(6073)$-C_{68} (as large as 151.0°) is noticeably more obtuse

than the corresponding angles in $Sc_2S@C_s(10528)$-C_{72} (125.36(14)°).[19] To the best of

our knowledge, it is the second most obtuse Sc-S-Sc angle among all characterized

di-scandium sulfide clusterfullerene, which is only smaller than that of

$Sc_2S@C_2(13333)$-C_{74}.[46]

Those two Sc-S bonds of $Sc_2S@C_{2v}(6073)$-C_{68} have equal lengths (2.30 Å)

which are shorter than the five other structures with Sc_2S units: 2.343 Å[20] (or 2.352

Å[21]) in $Sc_2S@C_2(7892)$-C_{70}, 2.325(3) and 2.347(3) Å in $Sc_2S@C_s(10528)$-C_{72},[19]

2.335(3) and 2.416(4) Å in $Sc_2S@C_{3v}(8)$-C_{82},[17] and 2.3525(8) and 2.3902(8) Å in

$Sc_2S@C_s(6)$-C_{82}[17]. The fact that the Sc-S bond lengths are noticeably short should be

rationalized by the rather small endohedral cage.

Very recently, Popov *et al.*[47] proposed a simple yet efficient model to mimic the

effect of a carbon cage by introducing small organic π-systems to the free metallic

cluster. When the Sc_2S cluster is taken into consideration, each of the scandium atoms

coordinate with a pentalene unit, forming a $Sc_2S(C_8H_6)_2$ structure. After the "molecule"

is unconstrainedly optimized, the Sc-S-Sc angle is 110° which is significantly smaller

than that of Sc_2S cluster encapsulated in the $C_{2v}(6073)$-C_{68} cage. On the other hand,

variation of the Sc-S-Sc angle from 95° to 180° does not lead to strong destabilization

of the structure with the energy maximally increase as slight as only 6 kJ/mol. In this viewpoint, it can be naturally inferred that the Sc-S-Sc angle as large as 151° in $Sc_2S@C_{2v}(6073)$-C_{68} should have few influences on its stability. Length of the two Sc-S bonds of the minimal free cluster is 2.411 Å, and the length fluctuation in the range of ±0.09 Å cannot lead to significant destabilization. Nevertheless, Sc-S distances in $Sc_2S@C_{2v}(6073)$-C_{68} (2.30 Å) are even shorter, which is not in the range of (2.411±0.09) Å, resulting in relatively large distortion energy. Thus, we can conclude that the Sc_2S cluster is some strained in the C_{68} cage. When it is encapsulated in a larger cage (*i.e.*, C_{70}, C_{74}, or C_{80}), distortion energies obviously decrease as a consequence of the elongation of Sc-S distances. This may be the reason why the yield of $Sc_2S@C_{68}$ is relatively lower than other di-scandium sulfide clusterfullerenes.

(HOMO–8) -6.86 eV   (HOMO–1) -5.43 eV   HOMO -5.15 eV

LUMO -3.61 eV   (LUMO+1) -3.05 eV
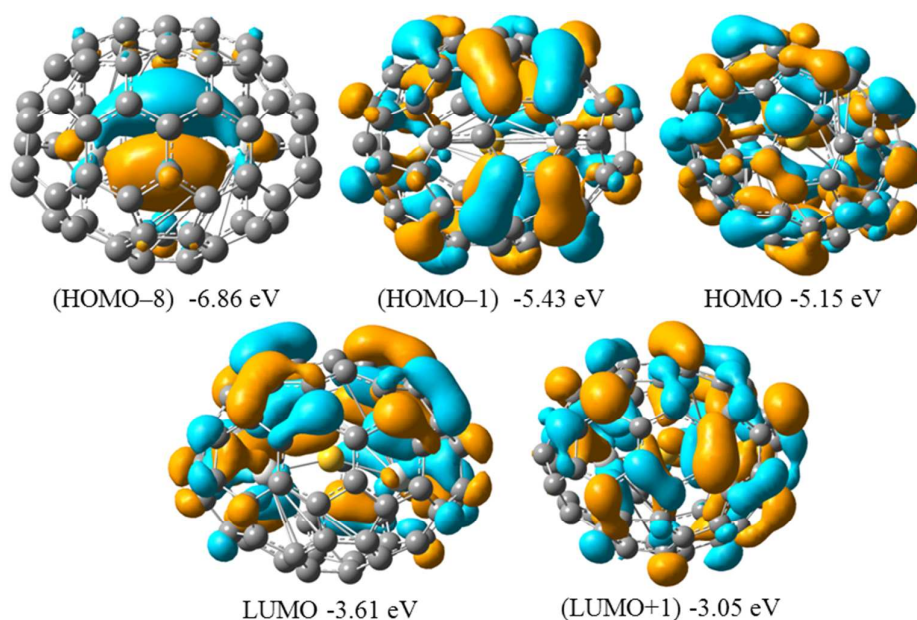
Figure 3. Five main frontier molecular orbitals (HOMO-8, HOMO-1, HOMO, LUMO, and LUMO+1) of $Sc_2S@C_{2v}(6073)$-C_{68}.

Five main frontier molecular orbitals of $Sc_2S@C_{2v}(6073)$-C_{68} including energy

levels are presented in Figure 3. It can be seen that HOMO – 8 (HOMO = the highest occupied molecular orbital) is mainly attributed from the metal cluster, and HOMO – 1 and HOMO are mainly located in the fullerene cage. More importantly, relatively substantial orbital overlaps between metallic atomic orbitals and cage orbitals exist in HOMO–1 and HOMO. As a result, covalent interactions between those two Sc atoms and pentalene units as well as between Sc and S atoms cannot be ignored (see part 3.3 for more details). Likewise, the LUMO (the lowest unoccupied molecular orbital) and LUMO+1 are also mainly attributed from cage orbitals with some important contributions of endohedral Sc_2S moiety. Therefore, redox reactions are predicted to take place on the fullerene cage primarily. Further confirmation of the conclusion has been performed by simulating spin densities of the oxidized and reduced $Sc_2S@C_{68}\_C_{2v}(6073)-C_{68}$, which discussed in ESI†.

The vertical electron affinity (VEA), vertical ionization potential (VIP) as well as adiabatic electron affinity (AEA) and adiabatic ionization (AIP) of $Sc_2S@C_{68}\_C_{2v}(6073)-C_{68}$ were computed respectively. the value of IP (VIP 6.31eV AIP 6.24 eV) is noticeably larger than that of $Sc_2S@C_2(7892)-C_{70}$ (6.00 eV),[20] $Sc_2S@C_{3v}(8)-C_{82}$ (5.10 eV) and $Sc_2S@C_s(8)-C_{82}$ (4.92 eV).[17] It indicates that the sulfide clusterfullerene is stable against oxidation. As for the value of EA (VEA -2.46 eV, AEA -2.56 eV) is more negative than that of $Sc_2S@C_2(7892)-C_{70}$ (-2.03 eV).[20] As a result, it suggests that $Sc_2S@C_{2v}(6073)-C_{68}$ is somewhat easier to take place reduction reactions. On the other hand, when a comparison is made between the EA of $Sc_2S@C_{68}\_C_{2v}(6073)-C_{68}$ and the two isomers of $Sc_2S@C_{82}$ (-3.61eV and -3.69 eV),

it seems that $Sc_2S@C_{2v}(6073)$-C_{68} is more stable to reduction reactions. To sum up, it can be concluded that the endofullerene $Sc_2S@C_{68}\_C_{2v}(6073)$-$C_{68}$ has good electron-accepting capacity but it is still stable in redox.

3.3 Bonding in $Sc_2S@C_{2v}(6073)$-C_{68}

As mentioned above, because of relatively substantial orbital overlaps between metallic atomic orbitals and cage orbitals, covalent interactions are significant in the $Sc_2S@C_{2v}(6073)$-C_{68}. To gain deep insight on its bonding natures, Mayer bond order[34-36] and bonding critical point (BCP) indicators of $Sc_2S@C_{2v}(6073)$-C_{68} are investigated in detail. A brief introduction to the BCP indicators derived from Bader's quantum theory of atoms in molecules (QTAIM)[37] have been stated in ESI†.
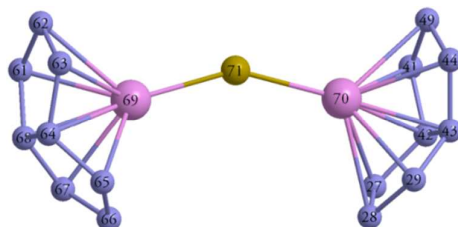
Figure 6. Serial numbers of Sc and S atoms in Sc_2S cluster as well as C atoms in those two pentalene moieties.

Utilizing MUlTIWFN 3.2.1 program,[38] Mayer bond orders of Sc-S and Sc-C bonds of $Sc_2S@C_{2v}(6073)$-C_{68} have been examined. Very recently, we employed the strategy to glance the interactions of two very large dimetallic carbide clusterfullerene, $Gd_2C_2@D_3(126408)$-C_{92} and $Gd_2C_2@C_1(126387)$-C_{92}, suggesting that covalent interactions of the two carbide clusterfullerenes should not be neglected.[28] The values of either Sc69-S71 or Sc70-S71 is over 1.0, which indicate that single bonds exist between Sc69 and S71 as well as Sc70 and S71. This is consistent with the fact that main contributions of (HOMO-8) come from the sulfide cluster. At the same time, the

Mayer bond order value between a scandium atom and one of carbon atoms of pentalene units is much smaller, revealing some weak covalent interactions in appearance. Interestingly, shown in Table 2 (also in Figure S9), the Mayer bond order values increase with decreasing Sc-C distance. Sc69-C64 and Sc69-C68 as well as Sc70-C42 and Sc70-C43 shows the largest Mayer bond orders which indicate the most significant covalent interactions between scandium atoms and the carbon cage. Clearly displayed in Figure 6, two (5,5)-bonds consist of those four carbon atoms. Moreover, bonding referring to transition metals is much more delocalized. For instance, Bader has shown that the bonding of Ti or Fe to a cyclopentadienyl ring is better described by bonding to a delocalized cone of electron density rather by individual localized Fe-C or Ti-C bonds.[48,49] Based on that, if we see the fused pentagon adjacencies as a whole, the orders of Sc bonding to a pentalene unit are as large as 1.527 (Sc69) and 1.526 (Sc70) respectively, indicating obvious covalent characters between Sc atoms and pentalene adjacencies.

Table 2. Mayer bond orders of Sc-S and Sc-C bonds as well as Sc-C bond lengths.

|		Mayer bond orders	d (Sc-C)			Mayer bond orders	d (Sc-C)
	C61	0.182	2.336		C27	0.196	2.337
	C62	0.178	2.418		C28	0.171	2.430
	C63	0.180	2.342		C29	0.199	2.325
	C64	0.210	2.263		C41	0.179	2.345
Sc69	C65	0.197	2.334	Sc70	C42	0.210	2.263
	C66	0.171	2.432		C43	0.211	2.258
	C67	0.198	2.329		C44	0.183	2.333
	C68	0.211	2.260		C49	0.177	2.419
	S71	1.045			S71	1.046	

[a] The unit of all Sc-C bond lengths (d (Sc-C)) is Å.

Bonding critical point (BCP) indicators based on quantum theory of atoms in molecules (QTAIM) are also employed to disclose the bonding features of

14

$Sc_2S@C_{2v}(6073)\text{-}C_{68}$. Up to now, only a few papers on interactions of EMFs contain the QTAIM method. Popov *et al.*[50] utilized the method to perform an exhaustive study on bonding in major classes of EMFs. Later, Jin et al.[51] also applied this method to investigate intracluster and metal-cage covalent interactions of an unusual Sc_3NC unit in three fullerene cages, namely C_{68}, C_{78}, and C_{80}. Herein, we employed this method to investigate covalent interactions in a dimetallic sulfide clusterfullerene system for the first time. As shown in Figure 7, no metal-metal BCPs are found, revealing that there is no metal-metal bond between those two scandium atoms. Meanwhile, there is a BCP between Sc69 and S71 as well as Sc70 and S71, and some parameters of the two BCPs are listed in Table 4. It can be seen that the two groups of parameters have no significant difference, which further proves that the two Sc-S bonds is equivalent. The electron density at all BCPs (ρ_{BCP}) is small, and its Laplacian ($\nabla^2\rho_{BCP}$) is positive. Similar situations have been found in two previous theoretical investigations on bonding natures of EMFs utilized QTAIM by Kobayashi and Nagase[52,53]. Popov and Dunsch[50] have pointed out that for transition metals $\nabla^2\rho_{BCP}$ values are usually positive, and ρ_{BCP} values are small due to the diffuse character of the electron distribution. On the other hand, covalent interactions between scandium and sulfur atoms can be confirmed by the negative energy densities (both of them are -0.015 a.u., shown in Table 3.) and relatively large ratios of absolute value of potential energy density to kinetic energy density ($>$1a.u.). Besides, both the Sc69-S71 and Sc70-S71 BCPs have a very small ellipticity of electron density which is very close to zero, indicating that both the two Sc-S bonds may have characteristic of a single bond.
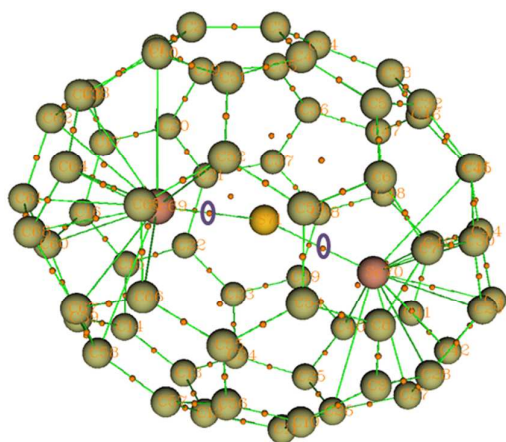
Figure 7. BCPs exist between Sc69 and S71 as well as Sc70 and S71. These two BCPs are highlighted by two violet rings surrounding them for clarity.

Table 3. BCPs' parameters for the Sc_2S cluster.[a]

Bond	ρ_{BCP}	$\nabla^2\rho_{BCP}$	H_{BCP}	$|V_{BCP}|/G_{BCP}$	ε
Sc69-S71	0.076	0.22	-0.015	1.21	0.033
Sc70-S71	0.076	0.22	-0.015	1.22	0.033

[a] The unit of all BCPs' parameters is a.u..

Next, we discuss the bonding nature between Sc_2S cluster and $C_{2v}(6073)$-C_{68} cage, which seems more intriguing. Shown in the Figure 8(*a*), surprisingly, there are at least four BCPs between the sulfur atom and carbon atoms in the cage; that is S71-C35 (BCP No. 93), S71-C13 (BCP No. 95), S71-C5 (BCP No. 99), and S71-C21 (BCP No. 90), of which some parameters have been collected in Table 4. It can be seen that all of the four BCPs have small and positive electron density, Laplacian of electron density, and energy density. Meanwhile, all four ratios of absolute value of potential energy density to kinetic energy density are less than 1. Those parameters demonstrate that it should be *van der Waals* interactions between the S atom and four C atoms in the cage. There are also at least four BCPs between two Sc atoms and four carbon atoms of which the two (5,5)-bonds consist: Sc69-C64, Sc69-C68, Sc70-C42, and Sc70-C43, as shown in Figure 8(*b*). Consequently, the two Sc atoms in the

16

present sulfide clusterfullerene mainly interact with the (5,5)-bonds of the cage, which is an ubiquitous feature for IPR-violating EMFs, and it corresponds to the fact that maximum Mayer bond order values exist between Sc atoms and those carbon atoms forming (5,5)-bonds. Parameters of the four BCPs listed in Table 4 suggest that similar metal-cage interactions exist in the four Sc-C bonds. Compared with the Sc-S BCPs, the electron density of Sc-C BCPs is slightly smaller than that of Sc-S BCPs, which may attribute to smaller electronegativity of a carbon atom. Fortunately, the energy density and ratios of absolute value of potential energy density to kinetic energy density are negative and relatively large ($>$1) respectively. Thus the bonding between the sulfide cluster and the C_{2v}(6073)-C_{68} cage can be classified as covalent interactions. In terms of larger ellipticities of electron density at Sc-C BCPs than those at Sc-S BCPs, it can be inferred characteristic of increasing π character of those four Sc-C bonds.[50]

(*a*)

(*b*)
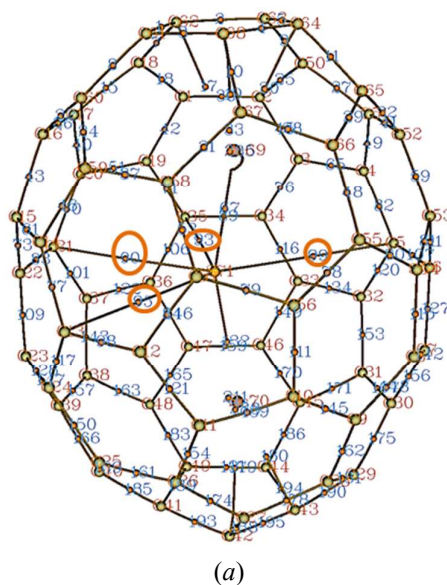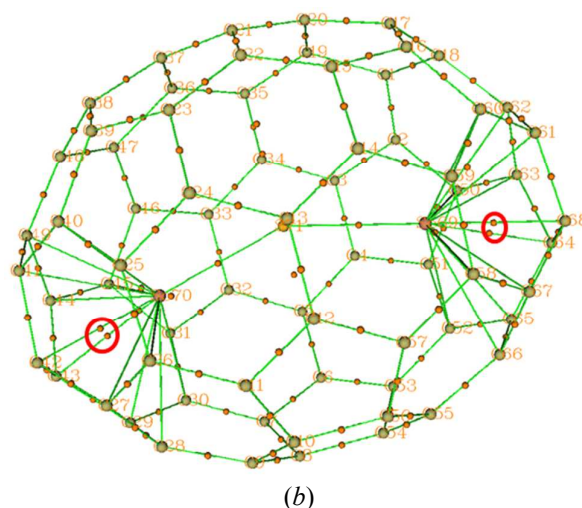
Figure8. Some important BCPs: (*a*) between S atom and four carbon atoms in the cage (highlighted by orange) and paths of those BCPs, (*b*) between Sc and carbon atoms in the pentalenes (highlighted by red). Series numbers of atoms and BCPs are colored by orange and blue respectively. Black and green sticks in (*a*) and (*b*) means BCP paths and form bonds respectively.

Table 4. BCPs' parameters for Sc_2S-cage interactions. [a]

Bond	ρ_{BCP}	$\nabla^2\rho_{BCP}$	H_{BCP}	$|V_{BCP}|/G_{BCP}$	ε
S71-C35	0.011	0.035	0.0013	0.824	0.014
S71-C13	0.0082	0.024	0.00090	0.824	1.19
S71-C5	0.00805	0.023	0.00087	0.820	1.18
S71-C21	0.011	0.035	0.0013	0.821	0.052
Sc69-C64	0.060	0.224	-0.0072	1.11	0.66
Sc69-C68	0.060	0.225	-0.0073	1.12	0.56
Sc70-C48	0.060	0.224	-0.0071	1.11	0.72
Sc70-C43	0.061	0.226	-0.0074	1.12	0.52

[a] The unit of all BCPs' parameters is a.u..

3.4 Electrochemical properties of $Sc_2S@C_{2v}(6073)$-C_{68}

In the year of 2006, Xu et al.[54] reported electrochemical behaviors of a series of ytterbium-containing metallofullerenes, providing a full electrochemical data set of metallofullerenes based on different cages. They proposed that cage structure plays an important role in determining the electronic properties. As a result, electrochemical properties of EMFs should be carefully investigated. Considering the low yields of $Sc_2S@C_{68}$, theoretical computation becomes important.

Table 5. Spin Multiplicities (*S*), relative energies [a] (ΔE, eV), and redox potentials (φ, V) of

$[Sc_2S@ C_{2v}(6073)\text{-}C_{68}]^q$ ($q = 0, \pm1,$ and ±2) in o-dichlorobenzene solvent (dielectric constant $=$ 10.12).

| q	-2	-1	0	+1	+2
S	1	2	1	2	1
ΔE	-7.93	-4.36	0.00	5.71	12.20
φ	-1.41	-0.62		0.73	1.51

$q = 0$ as the reference point of zero potential energy.

Calculated redox potentials of $Sc_2S@C_{2v}(6073)\text{-}C_{68}$ have been listed in Table 5. The first reduction peak (-0.62 V) of $Sc_2S@C_{2v}(6073)\text{-}C_{68}$ is positively shifted in comparison with those of $Sc_2S@C_2(7892)\text{-}C_{70}$ (-1.10 V)[20], $Sc_2S@C_{3v}(8)\text{-}C_{82}$ (-1.04 V) and $Sc_2S@C_s(6)\text{-}C_{82}$ (-0.98 V),[17] indicating that reduction reactions should somewhat easily take place upon $Sc_2S@C_{2v}(6073)\text{-}C_{68}$. On the other hand, the first oxidation peak (0.73 V) is noticeably larger than those of $Sc_2S@C_2(7892)\text{-}C_{70}$ (0.52 V) [20], $Sc_2S@C_{3v}(8)\text{-}C_{82}$ (0.52 V) and $Sc_2S@C_s(6)\text{-}C_{82}$ (0.39 V),[17] which means that the oxidation of $Sc_2S@C_{2v}(6073)\text{-}C_{68}$ is hard to take place.

3.5 ^{13}C NMR, UV-vis-NIR, and IR properties of $Sc_2S@C_{2v}(6073)\text{-}C_{68}$

Through the gauge-independent atomic orbital method, the chemical shifts were calculated at the B3LYP/6-31G(d)-Lanl2dz level of theory. The ^{13}C NMR spectra has been calculated and presented in Figure 6. Theoretical chemical shift values have been calibrated to the observed C_{60} line (143.15 ppm).[45] Since the endohedral fullerene still maintains the C_{2v} symmetry of the fullerene cage, $Sc_2S@C_{2v}(6073)\text{-}C_{68}$ is predicted to consist of 13 full intensity lines (4 carbons) and 8 half intensity lines (2 carbons), ranging from 134 to 157 ppm. The detailed calculated chemical shifts can be obtained in the Supporting Information.
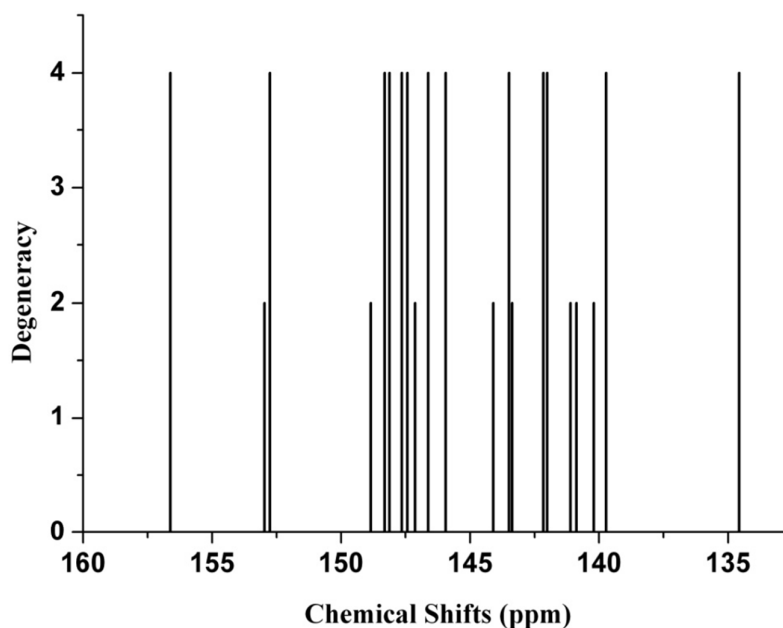
Figure 9. Simulated ^{13}C NMR spectrum of $Sc_2S@C_{2v}(6073)$-C_{68}.

By time-dependent density functional theory (TD-DFT), the UV-vis-NIR absorption spectrum of $Sc_2S@C_{2v}(6073)$-C_{68} has been calculated and shown in Figure 5. The main highlighted peaks have been labeled as 414, 509, 613, 723, 976 and 1323 nm. The characteristic peaks are substantially different from $Sc_3N@C_{68}$.[12] The highlighted peaks have been assigned to electronic transitions and are collected in the Supporting Information. With these characteristic peaks, $Sc_2S@C_{2v}(6073)$-C_{68} can be identified easily in experiment. The weak but broad absorption peak at 1323 nm is associated with the HOMO→LUMO excitation called the optical absorption gap, which corresponds to an energy gap of 0.94 eV. The second main absorption bond at 967 nm, even stronger than the one at 1323 nm, is attributed to the HOMO-1→LUMO transition with an energy gap of 1.28 eV. Another important absorption peak is at 723 nm mainly associated with the HOMO→LUMO+1 excitation with an energy gap of 1.71 eV. The other main absorption peaks are mainly attributed to the $\pi \rightarrow \pi^*$ excitation transitions of the fullerene cage.

20
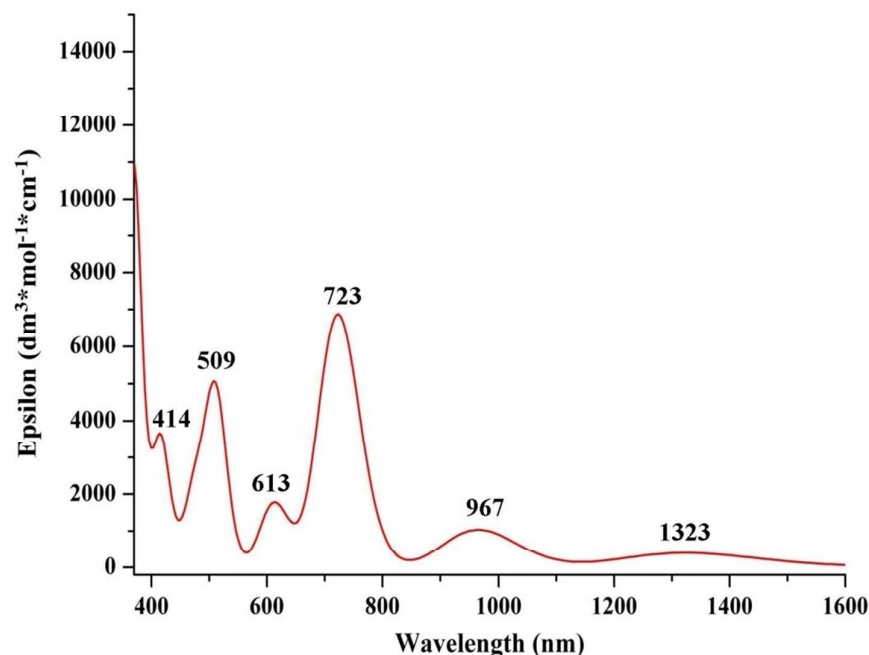
Figure 10. Simulated UV-Vis-NIR spectrum of $Sc_2S@C_{2v}(6073)$-C_{68}.

The IR spectrum of $Sc_2S@C_{2v}(6073)$-C_{68} have also been theoretically simulated

by harmonic vibrational analysis at B3LYP/3-21G*~Lanl2dz level of theory. As

shown in Figure 11, the IR spectrum can be mainly divided into three regions. The

lowest region with its wavenumber from 0-200 cm^{-1} is attributed to the frustrated

translation and rotation of the inner cluster, which is much weaker compared with

other two regions. As a consequence of large mass of the metallic ions of the Sc_2S

cluster the modes present rather low frequencies. The other two regions (200-1000

and 1000-1600 cm^{-1}) belong to the cage breathing corresponding C-C bond stretching

modes of the fullerene cage.[55] The important characteristic feature of that IR spectrum

is the ultra-high absorption peaks at 1355 and 1373 cm^{-1}, which may be utilized as the
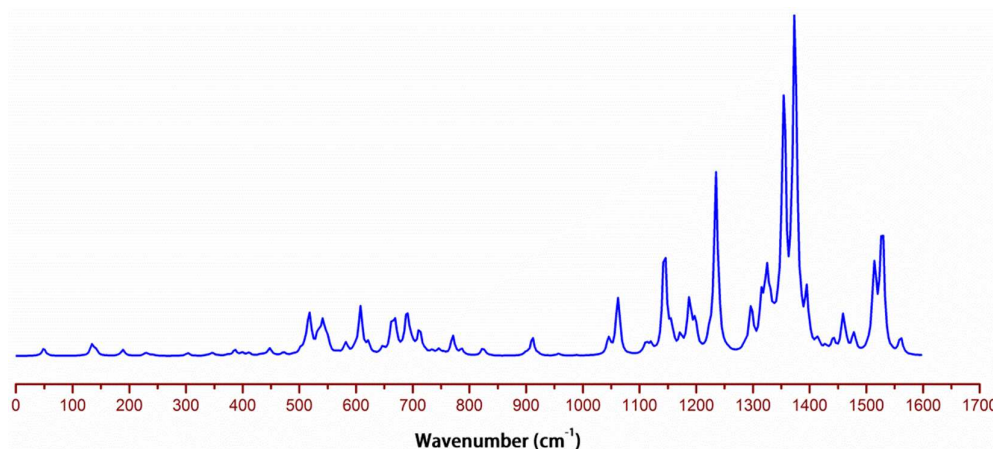
elucidation of the cage structure.

Figure 11. Simulated IR spectrum of $Sc_2S@C_{2v}(6073)-C_{68}$.

4. Conclusions

To summarize, by means of DFT combined with statistical thermodynamics calculations, the structure of mass spectrum detected smallest dimetallic sulfide EMFs $Sc_2S@C_{68}$ has been unambiguously confirmed. An obtuse discandium sulfide cluster with the Sc-S-Sc angle as large as 151° is encapsulated in the $C_{2v}(6073)-C_{68}$ cage with two opposite fused pentagon adjacencies. This $Sc_2S@C_{68}$ isomer owns the lowest relative potential energy as well as best thermodynamic stability, and quite large HOMO-LUMO gap. Frontier molecular orbital analysis of the isomer as well as spin density distribution of its single cation and anion reveals that redox reactions should mainly take place at fullerene cage rather than the inner cluster. Meanwhile, substantial overlaps between metallic orbitals and cage orbitals indicate strong coupling between the intracluster and cage. The covalent interactions of internal cluster as well as metal-cage have been characterized obviously in terms of Mayer bond order and BCP indicators derived from QTAIM. Two Sc-S single bonds form in the cluster, and the Sc atoms mainly bond to the (5,5)-bonds of the cage. Electrochemical properties, ^{13}C NMR, UV-vis-NIR and IR spectra have also been

22

simulated to assist future experimental characterization. This work has not only confirmed the structure of the smallest dimetallic sulfide clusterfullerene detected up to now, but also deepened the understanding of interactions between cluster and cage as well as atoms among trapped cluster.

Acknowledgements

References and Notes

1   A. A. Popov, S. Yang, L. Dunsch, *Chem. Rev.*, 2013, **113,** 5989.

2   P. W. Fowler, and D. E. Manoloupoulos, *An Atlas of Fullerenes*; Oxford University Press: Oxford, 1995.

3   C.-R. Wang, T. Kai, T. Tomiyama, T. Yoshida, Y. Kobayashi, E. Nishibori, M. Takata, M. Sakata, and H. Shinohara, *Nature*, 2000, **408,** 426.

4   H. Zheng, X. Zhao, W. W. Wang, T. Yang, and S. Nagase, *J. Chem. Phys.*, 2012 **137**, 014308.

5   Y. Feng, T. Wang, J. Wu, L. Feng, J. Xiang, Y. Ma, Z. Zhang, L. Jiang, C. Shu, and C. Wang, *Nanoscale,* 2013, **5,** 6704.

6   T. Yang, X. Zhao, S.-T. Li, and S. Nagase, *Inorg. Chem.*, 2012, **51,** 11223.

7   J. Zhang, F. L. Bowles, D.W. Bearden, W. K. Ray, T. Fuhrer, Y. Ye, C. Dixon, K. Harich, R. F. Helm, M. M. Olmstead, and A. L. Balch, *Nature Chem.*, 2013, **5,** 880.

8   M. M. Olmstead, H. M. Lee, J. C Duchamp, S. Stevenson, D. Marciu, H. C. Dorn, and A. L. Balch, *Angew. Chem.*, 2003, **115,** 928; *Angew. Chem. Int. Ed.*, 2003, **42,** 900.

9   J. U. Reveles, T. Heine, and A. M. Kçster, *J. Phys. Chem. A*, 2005, **109,** 7068.

10   J. M. Campanera, C. Bo, and J. M. Poblet, *Angew. Chem.*, 2005, **117,** 7396; *Angew. Chem. Int. Ed.*, 2005, **44,** 7230.

11   S. S. Park, D. Liu, and F. Hagelberg, *J. Phys. Chem. A*, 2005, **109,** 8865.

12   S. Yang, M. Kalbac, A. Popov, and L. Dunsch, *Chem. Eur. J.*, 2006, **12,** 7856.

13   S. Stevenson, P. W. Fowler, T. Heine, J. C. Duchamp, G. Rice, T. Glass, K. Harish, E. Harich, E. Hajdu, R. Bible, and H. C. Dorn, *Nature*, 2000, **408,** 427.

14   M. R. Cerón, F.-F. Li, and L. A. Echegoyen, *J. Phys. Org. Chem.*, 2014, **27,** 258.

15   Z.-Q. Shi, X. Wu, C.-R. Wang, X. Lu, and H. Shinohara, *Angew. Chem. Int. Ed.*, 2006, **45,** 2107.

16   L. Dunsch, S. Yang, L. Zhang, A. Svitova, S. Oswald, and A. A. Popov, *J. Am. Chem. Soc.*, 2010, **132,** 5413..

17   B. Q. Mercado, N. Chen, A. Rodríguez-Fortea, M. A. Mackey, S. Stevenson, L. Echegoyen, J. M. Poblet, M. M. Olmstead, and A. L. Balch, *J. Am. Chem. Soc.*, 2011, **133,** 6752.

18   N. Chen, M. N. Chaur, C. Moore, J. R. Pinzon, R. Valencia, A. Rodríguez-Fortea,

and J. M. Poblet, L. Echegoyen, *Chem. Commun.*, 2010, **46,** 4818.

19 N. Chen, C. M. Beavers, M. Mulet-Gas, A. Rodríguez-Fortea, E. J. Munoz, Y.-Y Li, M. M. Olmstead, A. L. Balch, J. M. Poblet, and L. Echegoyen, *J. Am. Chem. Soc.*, 2012, **134,** 7851.

20 T. Yang, X. Zhao, and S. Nagase, *Chem. Eur. J.*, 2013, **19,** 2649.

21 N. Chen, M. Mulet-Gas, Y.-Y. Li, R. E. Stene, C. W. Atherton, A. Rodríguez-Fortea, J. M. Poblet, and L. Echegoyen, *Chem. Sci.*, 2013, **4,** 180.

22 T. Pichler, Z. Hu, C. Grazioli, S. Legner, M. Knupfer, M. S. Golden, J. Fink, F. M. F. de Croot, M. R. C. Hunt, P. Rudolf, R. Follath, C. Jung, L. Kjeldgaard, P. Bruhwiler, M. Inakuma, and H. Shinihara, *Phys. Rev. B*, 2000, **62**, 13196.

23 M. J. S. Dewar, E. Zoebisch, E. F. Healy, and J. J. P. Stewart, *J. Am. Chem. Soc.*, 1985, **107,** 3902.

24 (a) A. D. Becke, *Phys. Rev. A*, 1988, **38,** 3098. (b) A. D. Becke, *J. Chem. Phys.*, 1993, **98,** 5648. (c) C. Lee, W. Yang, and R. G. Parr, *Phys. Rev. B: Condens. Matter Mater. Phys.*, 1988, **37,** 785.

25 P. J. Hay, and W. R. Wadt, *J. Chem. Phys.*, 1985, **82,** 299.

26 D. Andrae, U. Haussermann, M. Dolg, H. Stoll, and H. Preuss, *Theor. Chim. Acta*, 1990, **77,** 123.

27 X. Zhao, *J. Phys. Chem. B*, 2005, **109,** 5267.

28 Y.-J. Guo, T. Yang, S. Nagase, and X. Zhao, *Inorg. Chem.*, 2014, **53,** 2012.

29 T. Yang, X. Zhao, and E. Ōsawa, *Chem. Eur. J.*, 2011, **17,** 10230.

30 H. Zheng, X. Zhao, T. Ren, and W.-W. Wang, *Nanoscale,* 2012, **4,** 4530.

31 T. Yang, X. Zhao, and S. Nagase, *Phys. Chem. Chem. Phys.* 2011, **13,** 5034.

32 F. Uhlík, Z. Slanina, S.-L. Lee, T. Akasaka, and S. Nagase, *Phys. Status Solidi B*,
    2013, **250,** 2709.

33 Gaussian 09 (Revision A.01), M. J. Frisch, G. W. Trucks, H. B. Schlegel, G. E.
    Scuseria, M. A. Robb, J. R. Cheeseman, G. Scalmani, V. Barone, B. Mennucci, G.
    A. Petersson, H. Nakatsuji, M. Caricato, X. Li, H. P. Hratchian, A. F. Izmaylov, J.
    Bloino, G. Zheng, J. L. Sonnenberg, M. Hada, M. Ehara, K. Toyota, R. Fukuda, J.
    Hasegawa, M. Ishida, T. Nakajima, Y. Honda, O. Kitao, H. Nakai, T. Vreven, J. A.
    Montgomery, Jr., J. E. Peralta, F. Ogliaro, M. Bearpark, J. J. Heyd, E. Brothers, K.
    N. Kudin, V. N. Staroverov, R. Kobayashi, J. Normand, K. Raghavachari, A. J.
    Rendell, C. Burant, S. S. Iyengar, J. Tomasi, M. Cossi, N. Rega, J. M. Millam, M.
    Klene, J. E. Knox, J. B. Cross, V. Bakken, C. Adamo, J. Jaramillo, R. Gomperts, R.
    E. Stratmann, O. Yazyev, A. J. Austin, R. Cammi, C. Pomelli, J. W. Ochterski, R.
    L. Martin, K. Morokuma, V. G. Zakrzewski, G. A. Voth, P. Salvador, J. J.
    Dannenberg, S. Dapprich, A. D. Daniels, Ö. Farkas, J. B. Foresman, J. V. Ortiz, J.
    Cioslowski, and D. J. Fox, Gaussian, Inc., Wallingford CT, 2009.

34 I. Mayer, *Chem. Phys. Lett.*, 1983, **97,** 270.

35 I. Mayer, *Int. J. Quantum Chem.*, 1984, **26,** 151.

36 A. J. Bridgeman, G. Cavigliasso, L. R. Ireland, and J. Rothery, *J. Chem. Soc*.,
    Dalton Trans., 2001, 2095.

37 R. F. W. Bader, *Atoms in Molecules—A Quantum Theory*, Oxford University
    Press, Oxford, 1990.

38 T. Lu, and F. W. Chen, *J. Comp. Chem*., 2012, **33,** 580.

39 a) A. Klamt, and G. Schüürmann, *J. Chem. Soc. Perkin Trans*., 1993, **2,** 799; b) A. Klamt, V. Jonas, T. Bürger, J. Lohrenz, *J. Phys. Chem. A* 1998, **102,** 5074.

40 a) B. Delley, *J. Chem. Phys.* 1990, **92,** 508; b) B. Delley, *J. Chem. Phys.,* 2000, **113,** 7756. DMol3 is available as part of Materials Studio and Cerius2 by Accelrys Inc.

41 M. F. Ryan, J. R. Eyler, and D. E. Richardson, *J. Am. Chem. Soc.* 1992, **114,** 8611.

42 K. Tan, and X. Lu, *J. Phys. Chem. A*, 2006, **110,** 1171.

43 K. Tan, X. Lu, and C.-R. Wang, *J. Phys. Chem. B*, 2006, **110,** 11098.

44 P. Jin, Z. Zhou, C. Hao, Z. Gao, K. Tan, X. Lu, and Z. Chen, *Phys. Chem. Chem. Phys.,* 2010, **12,** 12442.

45 R. Taylor, J. P. Hare, A. K. Abdul-Sada, H. W. Kroto, *J. Chem. Soc. Chem. Commun.* 1990, 1423.

46 L.-H. Gan, Q. Chang, C. Zhao, and C.-R. Wang, *Chem. Phys. Lett.*, 2013, **570,** 121.

47 Q. Deng, and A. A. Popov, *J. Am. Chem. Soc.*, 2014, **136,** 4257.

48 F. Cortés-Guzmán, and R. F. W. Bader, *Coord. Chem. Rev.,* 2005, **249,** 633.

49 R. F. W. Bader, and C. F. Matta, *Inorg. Chem.,* 2001, **40,** 5603.

50 A. A. Popov and L. Dunsch, *Chem.–Eur. J.,* 2009, **15,** 9707.

51 P. Jin, Z. Zhou, C. Hao, Z. Gao, K. Tan, X. Lu, and Z. Chen, *Phys. Chem. Chem. Phys.,* 2010, **12,** 12442.

52 K. Kobayashi and S. Nagase, *Chem. Phys. Lett.,* 1999, **302,** 312.

53 K. Kobayashi and S. Nagase, *Chem. Phys. Lett.,* 2002, **362,** 373.

54 J. Xu, M. Li, Z. Shi, and Z. Gu, *Chem. Eur. J.,* 2006, **12,** 562.

55 A. A. Popov, *J. Comput. Theor. Nanosci.*, 2009, **6,** 292.

TOC
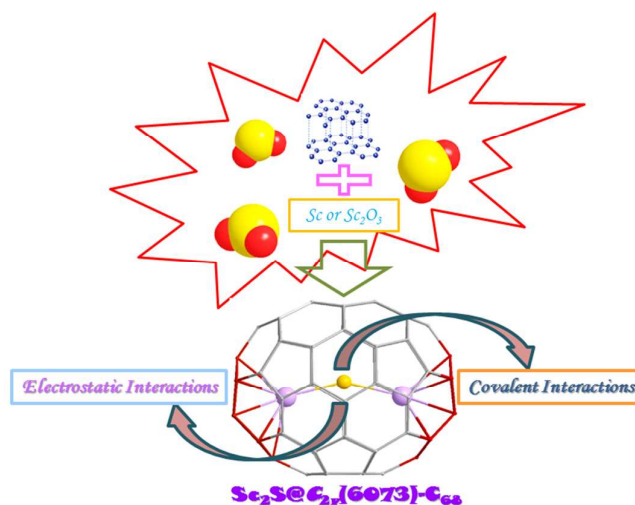
Density functional theory calculations combined with statistical thermodynamics treatments revealed that the mass spectrum detected $Sc_2S@C_{68}$ should possess the $C_{2v}(6073)$-C_{68} cage.